ORGANOMETALLICS
Article

Organometallics **2010,** *29,* 6509–6517 6509
DOI: 10.1021/om100850p

Sterically Hindered Diazabutadienes (DABs): Competing Reaction Pathways with MeLi

Mohan Bhadbhade,[†] Guy K. B. Clentsmith,*[,‡] and Leslie D. Field[‡]

[†]*University of New South Wales Analytical Centre and* [‡]*School of Chemistry, University of New South Wales, Sydney, New South Wales 2052, Australia*

Received September 2, 2010

Treatment of *N*,*N*′-bis(2,6-diisopropylphenyl)-1,4-diaza-2,3-dimethyl-1,3-butadiene with MeLi results in carbon−carbon bond formation and selective reduction of one of the imine arms to give the N-lithiated salt of the imine/amine, *N*,*N*′-bis(2,6-diisopropylphenyl)-1,4-diaza-2,3,3-trimethyl-1-butene. This compound crystallizes from Et_2O as a solvent adduct, exists as a monomer both in solution and the solid state, and features a three-coordinate lithium nucleus that is chelated to oxygen, amido, and imino donors. In contrast, treatment of *N*,*N*′-bis(2,4,6-trimethylphenyl)-1,4-diaza-2,3-dimethyl-1,3-butadiene with MeLi gives the N-lithiated imine anion *N*-(2,4,6-trimethylphenyl)-1-aza-2-methyl-3-*N*′-(2,4,6-trimethylphenyl)-1,3-butadiene, as the ether adduct, by proton abstraction. With a more hindered base, *N*,*N*′-bis(2,6-diisopropylphenyl)-1,4-diaza-2,3-dimethyl-1,3-butadiene undergoes proton abstraction with lithium diisopropylamide to give the N-lithiated imine anion of the ene/amine, *N*-(2,6-diisopropylphenyl)-1-aza-2-methyl-3-*N*′-(2,6-diisopropylphenyl)-1,3-butadiene, again isolated as the ether adduct. A further equiv of MeLi·LiBr added to *N*-(2,4,6-trimethylphenyl)-1-aza-2-methyl-3-*N*′-(2,4,6-trimethylphenyl)-1,3-butadiene gives the doubly N-lithiated salt of the diene/diamide, 2,3-*N*,*N*′-bis(2,4,6-trimethylphenyl)-1,3-butadiene, in which both nitrogen centers have been reduced, and which adopts a cisoid stereochemistry with respect to the butadiene unit in the solid state.

1. Introduction

1,4-Diaza-1,3-butadiene (DAB or α-diimine) ligands, when bound to middle- and late-transition-metal centers, boast an impressive array of reactivity[1] and sometimes impart useful catalytic activities in a variety of chemical transformations.[2] While some work points to the relative innocence of DAB ligands upon coordination, even in the presence of strong nucleophiles,[3] the ketimine moiety is nevertheless able to undergo reaction at any of the enolizable β-hydrogens and also at the electrophilic carbon of the imine group. This is also true for related multidentate ligands with ketimine donors such as the imino-substituted pyridines **2** and **3**,[4] where the pyridyl donors introduce another potentially reactive site in the heterocyclic ring.[5] In the context of olefin polymerization, such reactivity is often exploited to elaborate from the neutral precursor new anionic ligands,[4b] whose charge lends itself to subsequent reaction with Lewis acidic metal centers. For example, imine-based ligands **1**−**3** (typically Ar = 2,6-$Pr^i_2C_6H_3$, 2,4,6-$Me_3C_6H_2$) are methylated with 1 equiv of trimethylaluminum at the imine carbon with carbon−carbon bond formation to give an imine/amido system with geminal dimethyl groups (Scheme 1).[4] Likewise ligands such as ArN=CHCH=NAr (**1**) will undergo reactions with Lewis acidic metal alkyls $M(CH_2Ph)_4$ (M = Zr, Hf) to give an anionic imine/amido ligand bound in situ to the group 4 metal center.[6]

In the case of **1**, *N*,*N*′-(2,6-$Pr^i_2C_6H_3$)$_2$-1,4-diaza-1,3-butadiene, such reactivity gives rise to a chiral center at the point of addition;[4b] however, hydride migration from the adjacent position can occur to give an achiral species (Scheme 2).[1c]

(1) (a) Vrieze, K. *J. Organomet. Chem.* **1986**, *300*, 307–326. (b) van Koten, G.; Vrieze, K. *Adv. Organomet. Chem.* **1982**, *21*, 151–239. (c) Klerks, J. M.; Stufkens, D. J.; van Koten, G.; Vrieze, K. *J. Organomet. Chem.* **1979**, *181*, 271–283.

(2) (a) Gottfried, A. C.; Brookhart, M. *Macromolecules* **2003**, *36*, 3085–3100. (b) Grasa, G. A.; Singh, R.; Stevens, E. D.; Nolan, S. P. *J. Organomet. Chem.* **2003**, *687*, 269–279. (c) Heumann, A.; Giordano, L.; Tenaglia, A. *Tetrahedron Lett.* **2003**, *44*, 1515–1518. (d) Gottfried, A. C.; Brookhart, M. *Macromolecules* **2001**, *34*, 1140–1142. (e) Ittel, S. D.; Johnson, L. K.; Brookhart, M. *Chem. Rev.* **2000**, *100*, 1169–1203. (f) van Belzen, R.; Hoffmann, H.; Elsevier, C. J. *Angew. Chem., Int. Ed. Engl.* **1997**, *36*, 1743–1745.

(3) Bart, S. C.; Hawrelak, E. J.; Schmisseur, A. K.; Lobkovsky, E.; Chirik, P. J. *Organometallics* **2004**, *23*, 237–246.

(4) (a) Nienkemper, K.; Kehr, G.; Kehr, S.; Fröhlich, R.; Erker, G. *J. Organomet. Chem.* **2008**, *693*, 1572–1589. (b) Gibson, V. C.; Redshaw, C.; White, A. J. P.; Williams, D. J. *J. Organomet. Chem.* **1998**, *550*, 453–456. For the reaction between trimethylaluminum and the related acenapthene-1,2-bis-imine, see: (c) Tishkina, A. N.; Lukoyanov, A. N.; Morozov, A. G.; Fukin, G. K.; Lyssenko, K. A.; Fedushkin, I. L. *Russ. Chem. Bull., Int. Ed.* **2009**, *58*, 2250–2257.

(5) (a) Clentsmith, G. K. B.; Gibson, V. C.; Hitchcock, P. B.; Kimberley, B. S.; Rees, C. W. *Chem. Commun.* **2002**, 1498–1499. (b) Khorobkov, I.; Gambarotta, S.; Yap, G. P. A.; Budzelaar, P. H. M. *Organometallics* **2002**, *21*, 3088–3090.

(6) (a) De Waele, P.; Jazdzewski, B. A.; Klosin, J.; Murray, R. E.; Theriault, C. N.; Vosejpka, P. C.; Petersen, J. L. *Organometallics* **2007**, *26*, 3896–3899. For activation of diacetyl-based DAB ligands by Mn(II) hydrocarbyls see: (b) Riollet, V.; Coperet, C.; Basset, J. M.; Rousset, L.; Bouchu, D.; Grosvalet, L.; Perrin, M. *Angew. Chem., Int. Ed.* **2002**, *41*, 3025–3027. For activation of glyoxal-based DAB ligands by Group 3 metal hydrocarbyls see: (c) Kaneko, H.; Tsurugi, H.; Panda, T. K.; Mashima, K. *Organometallics* **2010**, *29*, 3463–3466.

Published on Web 11/02/2010

Scheme 1

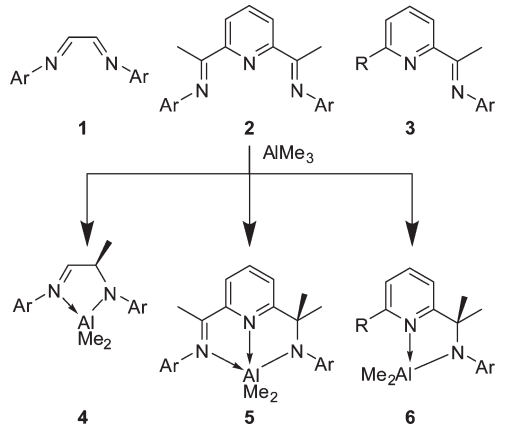

Scheme 2

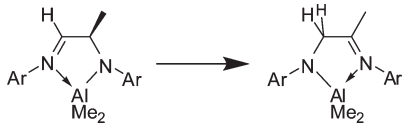

Scheme 3

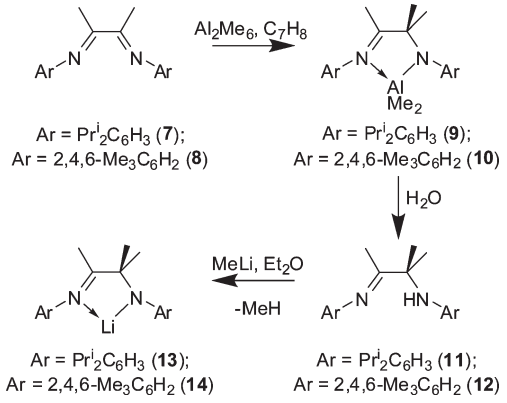

Related DAB ligands, N,N'-(2,6-$Pr^i_2C_6H_3$)$_2$-1,4-diaza-2,3-dimethyl-1,3-butadiene (**7**) and N,N'-(2,4,6-$Me_3C_6H_2$)$_2$-1,4-diaza-2,3-dimethyl-1,3-butadiene (**8**), are also reactive toward trimethylaluminum to give products analogous to **5** and **6**. For compound **7**, some of this chemistry has been reported in the patent literature (Scheme 3).[7] The methylated products **9** and **10** are readily hydrolyzed to give the parent imine/amines **11** and **12**, and lithiation by standard means allows for isolation of lithiated imine/amides **13** and **14**. Compounds **7** and **8** both have methyl groups attached to the imine carbon, and the pseudoallylic protons of the methyl substituents are susceptible to hydrogen abstraction by strongly basic reagents to give imine anions, a process which has some precedent in the chemistry of **2**[5b] and which features strongly in the chemistry of **8**. This means that there are competing reaction pathways that can occur when DAB compounds such as **7** and **8** are treated with reagents that are nucleophilic and/or basic.

While the DAB compounds **7** and **8** display similar reactivity toward trimethylaluminum, they undergo different reactions with MeLi. With the sterically more encumbered ligand, N,N'-(2,6-$Pr^i_2C_6H_3$)$_2$-1,4-diaza-2,3-dimethyl-1,3-butadiene (**7**), treatment with MeLi results in C−C bond formation and gives the lithiated imine/amide **13** directly. In contrast, the mesityl derivative N,N'-(2,4,6-$Me_3C_6H_2$)$_2$-1,4-diaza-2,3-dimethyl-1,3-butadiene (**8**) undergoes a stepwise deprotonation to give the singly reduced imine/ene-amide **15** and then the doubly reduced diene/diamide **16** after reaction with successive equivalents of MeLi (Scheme 4).

Scheme 4

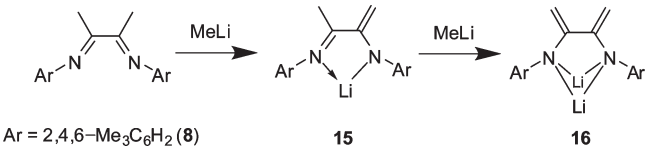

Single-crystal X-ray diffraction structures have been reported here for the lithiated compounds (2,6-$Pr^i_2C_6H_3$)N=C(Me)C(CH_3)$_2$N(Li)(2,6-$Pr^i_2C_6H_3$) (**13**), (2,4,6-$Me_3C_6H_2$)N=C(Me)C(=CH_2)N(Li)(2,4,6-$Me_3C_6H_2$) (**15**), and (2,4,6-$Me_3C_6H_2$)(Li)NC(=CH_2)C(=CH_2)N(Li)(2,4,6-$Me_3C_6H_2$)(LiBr)$_2$ (**16**), and for the compound (2,6-$Pr^i_2C_6H_3$)N=C(Me)C(=CH_2)N(Li)(2,6-$Pr^i_2C_6H_3$) (**17**) as well, which is the 2,6-diisopropylphenyl-substituted analogue of **15.** The structures of the dimethylaluminum derivatives (2,6-$Pr^i_2C_6H_3$)N=C(Me)C(CH_3)$_2$N($AlMe_2$)(2,6-$Pr^i_2C_6H_3$) (**9**) and (2,4,6-$Me_3C_6H_2$)N=C(Me)C(CH_3)$_2$N($AlMe_2$)(2,4,6-$Me_3C_6H_2$) (**10**) and that of the free amine (2,6-$Pr^i_2C_6H_3$)N=C(Me)C(CH_3)$_2$-N(H)(2,6-$Pr^i_2C_6H_3$) (**11**) will be reported elsewhere.[8]

2. Results and Discussion

The diazabutadiene precursors (2,6-$Pr^i_2C_6H_3$)N=C(Me)C(Me)=N(2,6-$Pr^i_2C_6H_3$) (**7**) and (2,4,6-$Me_3C_6H_2$)N=C(Me)C(Me)=N(2,4,6-$Me_3C_6H_2$) (**8**) can be synthesized in gram quantities by prolonged stirring of stoichiometric amounts of diacetyl with the appropriate aniline in methanol at room temperature. Small quantities of formic acid catalyze the condensation, and both DAB ligands precipitate from solution as yellow crystalline materials in high yields.[9] The 2,6-diisopropylphenyl-substituted compound **7** was recrystallized quantitatively from hot EtOH; the mesityl derivative **8**, which is much less soluble in alcohol, was washed with cold EtOH and used directly in further reactions.

The addition of 1−2 equiv of MeLi to (2,6-$Pr^i_2C_6H_3$)N=C(Me)C(Me)=N(2,6-$Pr^i_2C_6H_3$) (**7**) in Et_2O solution at ice-bath temperature rapidly discharged the yellow color of the starting material and generated an exotherm. The ^{1}H NMR spectrum of the reaction mixture in THF-d_8 results in quantitative formation of a C_s-symmetric product, as evidenced by the appearance of two sets each of aryl, methyl, and methine protons. The added MeLi reduces one of the donor arms of the starting ligand so that the halves of the molecule are differentiated in solution. The evidence that C−C bond formation has occurred includes (i) appearance of a singlet (6H integrand) at δ 1.30 ppm attributable to a *gem*-dimethyl group, (ii) the persistence of a methyl singlet at δ 1.81 ppm (3H) arising from the backbone methyl group of the unperturbed imine arm, and (iii) the absence of any

(7) Murray, R. E. US6562751 B2 20011218, 2002.

(8) Bhadbhade, M.; Clentsmith, G. K. B.; Field, L. D. Manuscript in preparation.

(9) (a) Türkmen, H.; Çetinkaya, B. *J. Organomet. Chem.* **2006**, *691*, 3749–3759. (b) tom Dieck, H.; Svoboda, M.; Greiser, T. *Z. Naturforsch., B: Chem. Sci.* **1981**, *36*, 823–832.

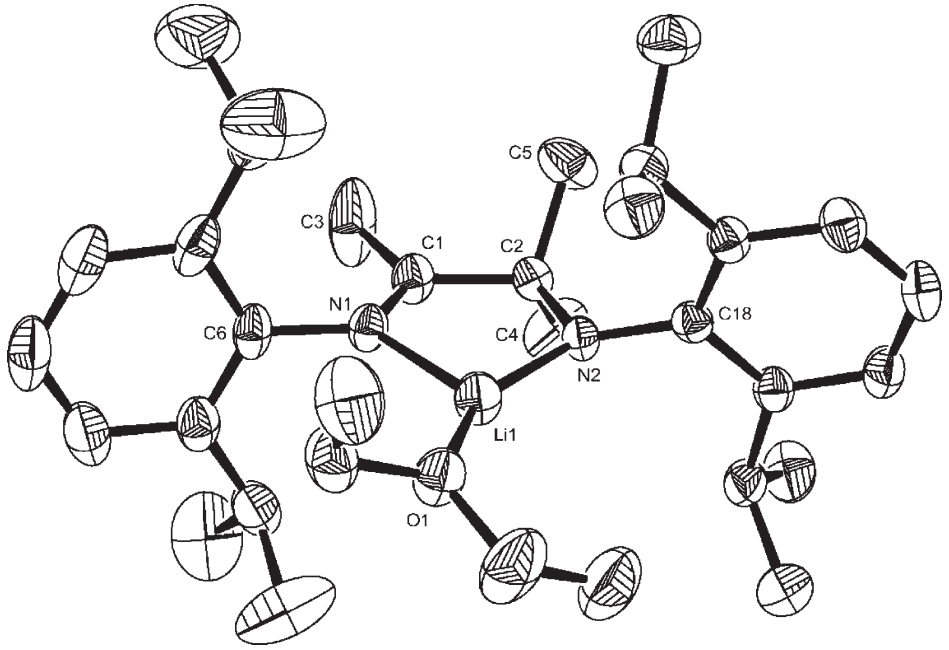

Figure 1. ORTEP representation of $[(2,6\text{-}Pr^i_2C_6H_3)N{=}C(Me)C(CH_3)_2N(Li)(2,6\text{-}Pr^i_2C_6H_3)]\cdot Et_2O$ (**13**$\cdot Et_2O$) with 50% probability ellipsoids. Hydrogen atoms have been omitted for clarity.

resonances attributable to vinylic protons, with the resulting reduction at a single imine function to give $(2,6\text{-}Pr^i_2C_6H_3)N{=}C(Me)C(CH_3)_2N(Li)(2,6\text{-}Pr^i_2C_6H_3)$ (**13**) (Scheme 3). The structure of **13** is also consistent with the appearance of singlets at δ 67.9 and 199.1 ppm in the $^{13}C\{^1H\}$ NMR spectrum in THF-d_8, and these resonances can be attributed to the quaternary carbon N$-C(Me_2)$ and $C{=}$N carbon nuclei in the structure. Yellow crystals of **13** were grown from Et_2O solution at -15 °C in 75−80% overall yields as the ether solvate, **13**$\cdot Et_2O$. C−C bond formation was unequivocally confirmed by a single-crystal X-ray diffraction experiment (Figure 1). Selected data appear in Table 1.

As seen in Figure 1, the lithium nucleus of $(2,6\text{-}Pr^i_2C_6H_3)N{=}C(Me)C(CH_3)_2N(Li)(2,6\text{-}Pr^i_2C_6H_3)$ (**13**$\cdot Et_2O$) is three-coordinate, with two longer coordinate-covalent bonds (Li−N1 = 1.977 Å, Li−O = 1.899 Å) and a covalent bond (Li−N2 = 1.858 Å). From the point of view of ligand structure, this is reasonable, given that it is this nitrogen that has been reduced with respect to the starting material by addition of a methyl group to the imine carbon and, therefore, it is this N2 center that is formally anionic. Significantly, **13**$\cdot Et_2O$ is a monomer in the solid state, and presumably the bulky aryl substituents, whose planes are canted normal to the plane containing the lithium nucleus and the donor atoms, act to suppress aggregation. C2−C4 (1.548 Å), C2−C5 (1.547 Å), and C2−N2 (1.458 Å) are all consistent with C−C or C−N single bonds, whereas the bond length C1−N1 (1.281 Å) is typical of a C=N double bond and is quite comparable with the C=N bond lengths measured in the structures of the precursor ligands **7**, and **8**.[10] The sums of the bond angles around the backbone C1 and C2 centers ($\sum_{\angle C1}$ = 360.0°, $\sum_{\angle C2}$ = 441.5°) also argue strongly for sp^2- and sp^3-hybridized carbon centers at C1 and C2, respectively.

The ^1H NMR spectrum of $(2,6\text{-}Pr^i_2C_6H_3)N{=}C(Me)C(CH_3)_2N(Li)(2,6\text{-}Pr^i_2C_6H_3)$ (**13**$\cdot Et_2O$) in THF-d_8, after recrystallization from Et_2O, highlights the diastereotopic nature of the methyl groups of the 2,6-diisopropyl substituents on the aniline rings. The isopropyl methyls of the aryl substituents on the amide side of the reduced DAB system

Table 1. Selected Bond Lengths (Å) and Bond Angles (deg) for $(2,6\text{-}Pr^i_2C_6H_3)N{=}C(Me)C(CH_3)_2N(Li)(2,6\text{-}Pr^i_2C_6H_3)$ (13**$\cdot Et_2O$), $(2,4,6\text{-}Me_3C_6H_2)N{=}C(Me)C(=CH_2)N(Li)(2,4,6\text{-}Me_3C_6H_2)$ (**15**$\cdot Et_2O$), $(2,4,6\text{-}Me_3C_6H_2)(Li)NC(=CH_2)C(=CH_2)N(Li)(2,4,6\text{-}Me_3C_6H_2)$ (**16**$\cdot 3Et_2O\cdot 2LiBr$), and $(2,6\text{-}Pr^i_2C_6H_3)N{=}C(Me)C(=CH_2)N(Li)(2,6\text{-}Pr^i_2C_6H_3)$ (**17**$\cdot Et_2O$)**

	13	**15**	**16**	**17**
		Bond Lengths		
Li1−N1	1.977(5)	1.912(10)	2.128(6)	1.907(5)
Li2−N1			1.955(5)	
Li1−N2	1.858(5)	1.956(9)		1.989(4)
Li1−O1	1.899(5)	1.904(8)	1.968(4)	1.911(7)
Li3−O2			1.943(5)	
C1−N1	1.281(3)	1.342(6)	1.371(3)	1.362(12)
C2−N2	1.458(3)	1.317(7)		1.257(13)
C1−C2	1.521(3)	1.488(7)	1.366(4)	1.544(14)
C1−C3	1.503(3)	1.408(7)		1.385(13)
C2−C4	1.549(4)	1.448(7)		1.558(14)
C2−C5	1.547(4)			
N1−$C_{ipso\text{-}aryl}$	1.432(3)	1.416(6)	1.423(3)	1.425(13)
N2−$C_{ipso\text{-}aryl}$	1.403(3)	1.427(6)		1.420(13)
C1−C1′			1.522(5)	
Li3−C2			2.319(3)	
Li3−Br1			2.512(5)	
Li3−Br2			2.578(5)	
Li2−Br2″			2.388(3)	
		Bond Angles		
N1−Li1−O1	122.4(2)	137.2(6)	127.3(5)	137.27(12)
N2−Li1−O1	139.0(3)	135.3(5)		135.44(12)
N1−Li1−N2	87.38(19)	86.9(4)		85.61(9)
N1−Li1−N1′			75.0(2)	
N1−Li2−N1′			83.0(3)	
C2−C1−C3	118.3(2)	119.2(5)		119.4(10)
C2−C1−C1′			121.35(17)	

(10) (a) Schaub, T.; Radius, U. *Z. Anorg. Allg. Chem.* **2006**, *632*, 807–813. (b) Cope-Eatough, E. K.; Mair, F. S.; Pritchard, R. G.; Warren, J. E.; Woods, R. J. *Polyhedron* **2003**, *22*, 1447–1454.

Scheme 5

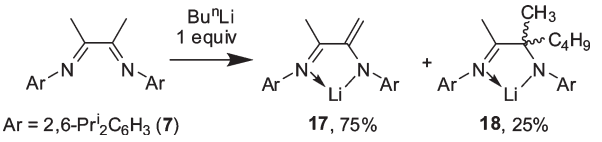

Scheme 6

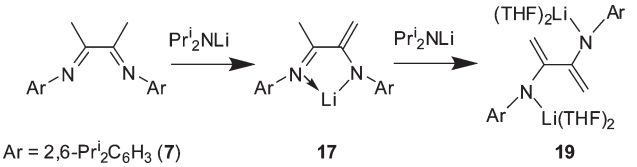

give rise to a pair of doublets at δ 1.20 and 1.12 ppm (12H) and at δ 1.30 and 1.28 ppm (12H) for the imine side of the reduced DAB. In addition to two signals for the aryl protons of each donor arm, the spectrum also exhibits two clearly distinct septet absorptions due to the methine protons of the isopropyl group at δ 4.23 and 3.06 ppm (4H, ^3J = 6.8 Hz). The upfield absorption corresponds to the methine proton on the imine side of the reduced DAB. Resonances attributable to the ether of crystallization (δ 3.39 ppm, q, 4H; δ 1.10, t, ^3J = 6.9 Hz, 6H) are also observed in the ^{1}H NMR spectrum. In previous examples of carbo-metalations of diketimines, the presence of stereocenters on the carbon backbone indicates the molecularity in solution.[4b,11] Thus, the Bu^{t}Li adduct of *N*,*N*′-(Bu^t)$_2$-1,4-diaza-1,3-butadiene, a dimer in the solid state, preserves this structure in benzene solution as the diastereomers observed in solution are necessarily aggregated.[11] Likewise, the aluminum compound **4** (Ar = 2,6-Pr$^i_2$), which is a monomer in the solid state, does not aggregate in solution, as argued by the absence of features attributable to diastereomers in its solution ^{1}H NMR spectrum.[4b]

The observation that the lithium derivative (2,6-Pr$^i_2$C$_6$H$_3$)N=C(Me)C(CH$_3$)$_2$N(Li)(2,6-Pr$^i_2$C$_6$H$_3$) (**13**) may be generated in usable yields by the simple addition of MeLi to the DAB compound (2,6-Pr$^i_2$C$_6$H$_3$)N=C(Me)C(Me)=N(2,6-Pr$^i_2$C$_6$H$_3$) (**7**) in Et$_2$O is remarkable. While addition of 2 equiv of MeLi is known to accomplish double reduction (i.e., dual carbo-lithiation) of less substituted DAB ligands such as *N*,*N*′-(Bu^t)$_2$-1,4-diaza-1,3-butadiene,[11] the more highly substituted, diacetyl-based diketimines rarely undergo nucleophilic addition with C−C bond formation, and under equivalent conditions, MeLi merely abstracts one of the backbone β-hydrogens of pyridyl imines such as **2** and **3** to give methane and the lithiated imine/ene-amide in an acid−base reaction.[5b,12] Likewise, addition of a stoichiometric amount of Bu^{n}Li to **7** in Et$_2$O affords low yields of the related, racemic lithiated imine/amide **18**, whose structure appears in the Supporting Information and in which the lithium reagent simply adds as a nucleophile to accomplish C−C bond formation (Scheme 5); quantities of the product of proton abstraction, (2,6-Pr$^i_2$C$_6$H$_3$)N=C(Me)C(=CH$_2$)N(Li)(2,6-Pr$^i_2$C$_6$H$_3$) (**17**), are also observed as the major product in the reaction mixture.

While MeLi adds to the imine with C−C bond formation, the methyl protons of (2,6-Pr$^i_2$C$_6$H$_3$)N=C(Me)C(Me)=N(2,6-Pr$^i_2$C$_6$H$_3$), (**7**) can be abstracted quantitatively if a nonnucleophilic base such as Pr$^i_2$NLi is used, and the resultant singly deprotonated species (2,6-Pr$^i_2$C$_6$H$_3$)N=C(Me)C(=CH$_2$)N(Li)(2,6-Pr$^i_2$C$_6$H$_3$) (**17**) was recrystallized from Et$_2$O in high yield. When **7** was treated with 2 equiv of Pr$^i_2$NLi in THF, deprotonation of both methyl groups occurred to give the known, symmetrical diene/diamide [(2,6-Pr$^i_2$C$_6$H$_3$)NC(=CH$_2$)C(=CH$_2$)N(2,6-Pr$^i_2$C$_6$H$_3$)]$^{2-}$Li$^+_2$·4THF (**19**) (Scheme 6).[13]

On the other hand, reduction of (2,6-Pr$^i_2$C$_6$H$_3$)N=C(Me)C(Me)=N(2,6-Pr$^i_2$C$_6$H$_3$) (**7**) with Li, Mg, or Na metal in THF or Et$_2$O gives moderate yields of [ArN(CH$_3$)C=C(CH$_3$)NAr]$^{2-}$M$^+_2$ (M = Li, Na) or [ArN(CH$_3$)C=C(CH$_3$)-NAr]$^{2-}$Mg^{2+}, in which both imine groups have been reduced but the central C−C bond has been oxidized to form an olefinic bond.[14] The putative 1,2-diamine ArN(H)C(CH$_3$)$_2$C-(CH$_3$)$_2$N(H)Ar, in which both imine donors have been reduced and both amino groups are protected by adjacent geminal dimethyl groups, has yet to be synthesized.

The lithiated imine/ene-amide (2,6-Pr$^i_2$C$_6$H$_3$)N=C(Me)C-(=CH$_2$)N(Li)(2,6-Pr$^i_2$C$_6$H$_3$) (**17**) was characterized by its ^{1}H NMR spectrum in THF-d_8. The molecule is unsymmetrical, and there are clearly two vinylic signals at δ 3.94 and 3.14 ppm (2H) correlated to signals at δ 78.0 (*C*=*C*H$_2$), and δ 59.1 ppm (*C*=CH$_2$) in the ^{13}C{^{1}H} NMR spectrum. The structure of **17**·Et$_2$O was obtained by single-crystal X-ray diffraction and appears in Figure 2. Selected structural data are given in Table 1.

The structure of **17**·Et$_2$O is monomeric, with the bulky aryl arms again perpendicular to the plane of the lithium−nitrogen core. Bond distances C4−C2 (1.479 Å) and C3−C1 (1.352 Å) clearly represent a C−C single bond and a double bond, respectively, as anticipated for an imine/ene-amide structure. The C−N bond distances reinforce these metrics (C2−N2 = 1.262 Å, C1−N1 = 1.315 Å), which clearly reflect an imine bond and a C−N single bond, respectively; the C1−N1 single bond is attached to the C3−C1 methylene unit, and conversely the C2−N2 double bond connects to the C4−C2 single bond, in accord with its simple formula representation.

Under conditions identical with those for the synthesis of (2,6-Pr$^i_2$C$_6$H$_3$)N=C(Me)C(CH$_3$)$_2$N(Li)(2,6-Pr$^i_2$C$_6$H$_3$) (**13**) from **7**, when *N*,*N*′-(2,4,6-Me$_3$C$_6$H$_2$)$_2$-1,4-diaza-2,3-dimethyl-1,3-butadiene (**8**) is treated with MeLi, C−C bond formation occurs and MeLi acts simply as a strong base to abstract one of the backbone methyl protons to give methane and the lithium-bound ene-amide (2,4,6-Me$_3$C$_6$H$_2$)N=C(Me)C-(=CH$_2$)N(Li)(2,4,6-Me$_3$C$_6$H$_2$) (**15**), with a coordinated imine arm (Scheme 7). As anticipated, the same product is isolated when **8** is treated with Pr$^i_2$NLi.

The structure of the resultant imine/ene-amide (2,4,6-Me$_3$C$_6$H$_2$)N=C(Me)C(=CH$_2$)N(Li)(2,4,6-Me$_3$C$_6$H$_2$) (**15**·Et$_2$O)

(11) (a) Gardiner, M. G.; Raston, C. L. *Inorg. Chem.* **1995**, *34*, 4206–4212. For other examples of carbo-metalation of bis-imines by lithium or magnesium reagents see: (b) Fedushkin, I. L.; Hummert, M.; Schumann, H. *Eur. J. Inorg. Chem.* **2006**, 3266–3273. (c) Fedushkin, I. L.; Makarov, V. M.; Rosenthal, E. C. E.; Fukin, G. K. *Eur. J. Inorg. Chem.* **2006**, 827–832. (d) Neumann, W. L.; Rogic, M. M.; Dunn, T. J. *Tetrahedron Lett.* **1991**, *32*, 5865–5868. (e) Stamp, L.; tom Dieck, H. *J. Organomet. Chem.* **1984**, *277*, 297–309.

(12) Nückel, S.; Burger, P. *Organometallics* **2000**, *19*, 3305–3311.

(13) Yu, L. B.; Yao, Y. M.; Shen, Q.; Sun, J. *Inorg. Chem. Commun.* **2004**, *7*, 542–544.

(14) (a) Mahrova, T. V.; Fukin, G. K.; Cherkasov, A. V.; Trifonov, A. A.; Ajellal, N.; Carpentier, J. F. *Inorg. Chem.* **2009**, *48*, 4258–4266. (b) Liu, Y.; Yang, P. J.; Yu, J.; Yang, X. J.; Zhang, J. D.; Chen, Z. F.; Schaefer, H. F.; Wu, B. *Organometallics* **2008**, *27*, 5830–5835.

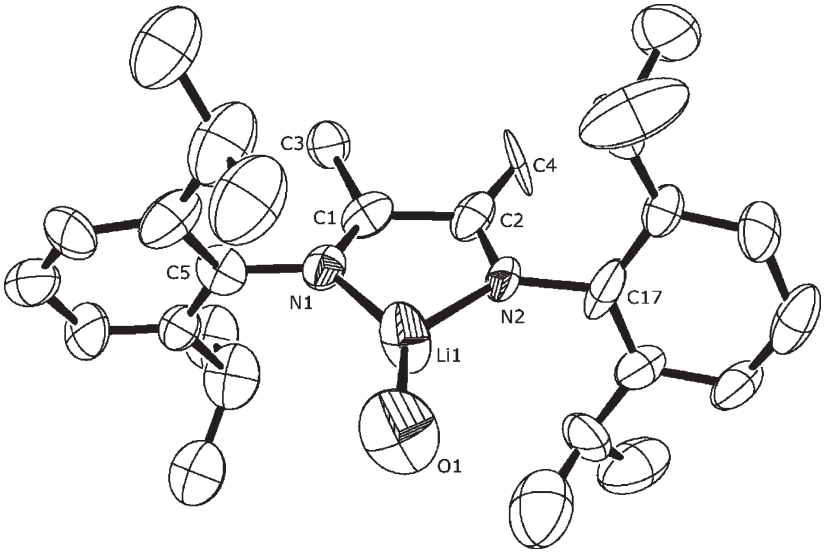

Figure 2. ORTEP representation of (2,6-$Pr^i_2C_6H_3$)N=C(Me)C(=CH_2)N(Li)(2,6-$Pr^i_2C_6H_3$) (**17**·Et_2O) with 50% probability ellipsoids. Disordered ethyl groups bound to the oxygen atom and hydrogen atoms have been omitted for clarity.

Scheme 7

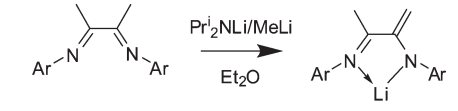

Ar = 2,4,6-$Me_3C_6H_2$ (**8**) **15**

is shown in Figure 3. This structure again features a discrete monomer whose lithium metal is again three-coordinate with a capping Et_2O molecule ($\sum_{\angle Li-O/N}$ = 359.6°). Here, the identity of single and double bonds is less apparent than in the other structures; however, the sum of the bond angles around the backbone carbons, C1 and C2, clearly point to sp^2-hybridized centers ($\sum_{\angle C1}$ = 360.0°, $\sum_{\angle C2}$ = 359.9°). The carbon−nitrogen bond distances (C1−N1 = 1.341(7) Å, C2−N2 = 1.318(6) Å) are barely differentiated, as are the lithium−nitrogen and the carbon−carbon distances (Li−N1 = 1.911(10) Å, Li−N2 = 1.956(10) Å; C1−C2 = 1.488(7) Å, C1−C3 = 1.408(7) Å; C2−C4 = 1.448(7) Å). Nevertheless, from these data it is clear that the N2−C2 and C1−C3 linkages represent a pair of conjugated double bonds and that it is the N1 center that is the formal anion. Unsaturation is more evident from the solution data, where the ^{1}H NMR spectrum exhibits a pair of vinylic protons at δ 3.79 and 2.97 ppm (2H) and the $^{13}C\{^1H\}$ NMR spectrum features a downfield singlet at δ 176.6 ppm, consistent with the imino carbon. Likewise, signals due to the ortho and para methyl groups of the mesityl rings (δ 2.14 and 2.04 ppm, 12H; δ 2.24, 1.92 ppm, 6H) as well as the unperturbed methyl group (C4) at δ 2.15 ppm are also clearly distinguishable in the ^{1}H NMR spectrum.

When (2,4,6-$Me_3C_6H_2$)N=C(Me)C(Me)=N(2,4,6-$Me_3C_6H_2$) (**8**) was treated with >2 equiv of MeLi·LiBr in Et_2O (or, alternatively, when a further 1 equiv of MeLi·LiBr was added to (2,4,6-$Me_3C_6H_2$)N=C(Me)C(=CH_2)N(Li)(2,4,6-$Me_3C_6H_2$) (**15**)), stoichiometric proton abstraction occurred to give the dilithiated diamido/diene (2,4,6-$Me_3C_6H_2$)-(Li)NC(=CH_2)C(=CH_2)N(Li)(2,4,6-$Me_3C_6H_2$) (**16**), with a cisoid structure in the solid state (Scheme 8). This compound has the formulation **16**·3Et_2O·2LiBr and comprises a polymeric structure, in which a terminal lithium nucleus (Li2) is loosely bound to the bromide nucleus (Br2″) of an adjacent formula unit, as shown in Figure 4. The C1−C2 bond length is 1.365(4) Å, which is consistent with an olefinic bond. On the other hand, the C1−C1′ (1.522 Å) and C1−N1 (1.373 Å) bond lengths clearly represent single bonds. The subsidiary LiBr units, whose origin is easily traced to the LiBr present in the ethereal solution of the MeLi used to prepare this species, interact loosely with the methylene units of the backbone (C2−Li3 = 2.319 Å) and act to bridge the formula units with the unsolvated lithium nucleus, Li2, acting as the junction (Li2−Br2″ = 2.388(3) Å). In solution, while there is no way to determine the molecularity of this species, the observed ^{1}H NMR signals clearly point to a species with C_s geometry, as suggested by the crystallographic symmetry: one set of aryl protons (δ 6.62 ppm, 4H) and two distinct vinyl resonances (δ 3.08, 2.13 ppm, 4H), and methyl resonances (δ 2.19, 2.14 ppm, 18H) are observed, along with resonances due to the ether of crystallization. The ^{7}Li NMR spectrum of **16**·3Et_2O·2LiBr reveals several chemically distinct lithium environments at low temperature; however, it has not been possible to establish their identities. If lithium reagents without stoichiometric LiBr are employed in reaction with **8** (i.e., if bromide-free MeLi is used), signals attributable to **16** can be observed in the ^{1}H NMR spectrum; however, crystalline material has not been isolated.

The two diazabutadienes (2,6-$Pr^i_2C_6H_3$)N=C(Me)-C(Me)=N(2,6-$Pr^i_2C_6H_3$) (**7**) and (2,4,6-$Me_3C_6H_2$)N=C(Me)C(Me)=N(2,4,6-$Me_3C_6H_2$) (**8**) thus follow different paths when treated with MeLi. For **7**, nucleophilic attack occurs at the imine carbon, whereas with **8**, proton abstraction occurs at the methyl group attached to the imine carbon. Both of these reaction pathways are not unreasonable, and since MeLi is potent as both a base and a nucleophile, the reactions with MeLi are probably under kinetic control linked to the ease of proton abstraction. With both **7** and **8**, the product of reaction contains a five-membered, unsaturated ring with lithium bound to amido, imino, and oxygen donors; therefore, the thermodynamic course of each

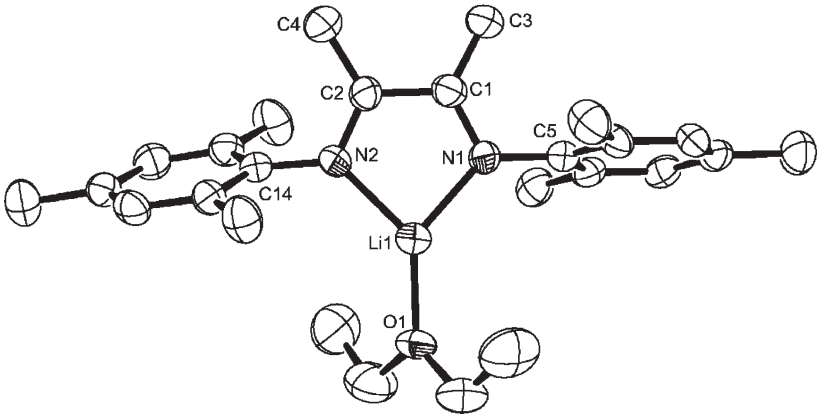

Figure 3. ORTEP representation of (2,4,6-$Me_3C_6H_2$)N=C(Me)C(=CH_2)N(Li)(2,4,6-$Me_3C_6H_2$) (**15**·Et_2O), with 50% probability ellipsoids. Hydrogen atoms have been omitted for clarity.

Scheme 8

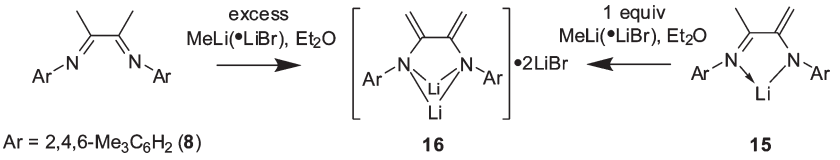

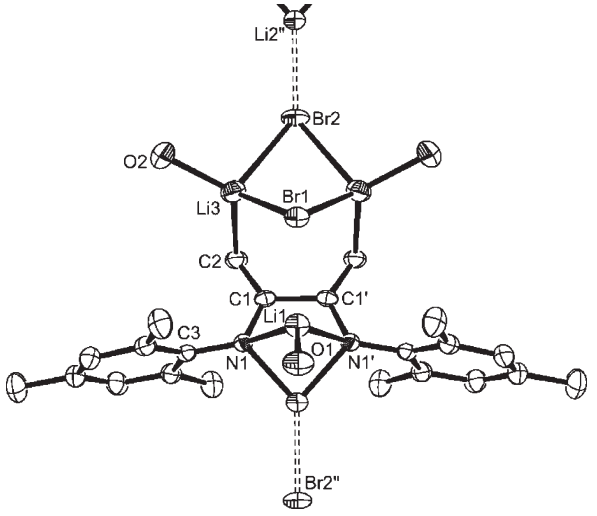

Figure 4. ORTEP representation of (2,4,6-$Me_3C_6H_2$)(Li)NC(=CH_2)C(=CH_2)N(Li)(2,4,6-$Me_3C_6H_2$) (**16**·3Et_2O·2LiBr) with 50% probability ellipsoids. Hydrogen atoms and ethyl groups attached to oxygen have been omitted for clarity.

reaction is reasonably similar. Little data exist on the pK_a values of simple imines and aldimines,[15] and there are no data for the diketimines studied in this work. A more recent study of imine metalation,[16] which dealt solely with lithium dialkylamides as the basic reagent but which also considered the effect of chelation of the alkali metal by pendant groups on the starting imine, concluded that increased steric bulk around the starting imine raised activation enthalpies with respect to proton abstraction and metalation. Thus, while the bulkier isopropyl substitution on **7** sterically shields the imine carbon from prospective attack by a nucleophile, the

Scheme 9

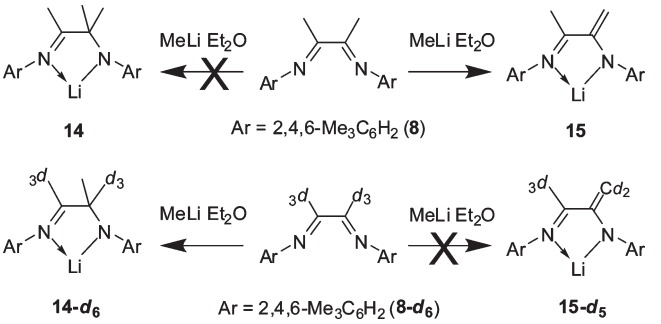

electron-releasing substitution on the aryl group acts to decrease the acidity of the hydrogens on the methyl substituent on the imine carbon.

To test this proposal, the deuterium-labeled starting material (2,4,6-$Me_3C_6H_2$)N=C(Me-d_3)C(Me-d_3)=N(2,4,6-$Me_3C_6H_2$) (**8**-d_6) was prepared from diacetyl-d_6 and mesitylaniline. *protio*-Diacetyl undergoes slow deuteration in D_2O at reflux with a trace of DCl, and the degree of deuteron incorporation was increased by several cycles at reflux.[17] Upon condensation with mesitylaniline in methyl alcohol-*d* in the presence of catalytic formic acid-*d*,[3] **8**-d_6 was obtained in reasonable purity (approximately 85%, as determined by integration of the ^{1}H NMR spectrum in benzene-d_6). Significantly, the reaction of **8**-d_6 with 1 equiv of MeLi in Et_2O at ice-bath temperature proceeds with no loss of intensity of the yellow color of the ketimine starting material, as occurs when *protio*-**8** is treated with this reagent. Yellow crystals of (2,4,6-$Me_3C_6H_2$)N=C(Me-d_3)C(Me-d_3)(Me)N(Li)(2,4,6-$Me_3C_6H_2$) (**14**-d_6·Et_2O) were obtained from THF/hexanes in moderate yield, and the solution spectroscopic data are entirely consistent with the product of carbon−carbon bond formation (Scheme 9). In THF-d_8 solution, **14**-d_6·Et_2O displays (i) two signals for

(15) Fraser, R. R.; Bresse, M.; Chuaqui-Offermanns, N.; Houk, K. N.; Rondan, N. G. *Can. J. Chem.* **1983**, *61*, 2729–2734.
(16) Romesberg, F. E.; Collum, D. B. *J. Am. Chem. Soc.* **1995**, *117*, 2166–2178.
(17) Plouzennec-Houe, I.; Lemberton, J. L.; Perot, G.; Guisnet, M. *Synthesis* **1983**, 659–661.

the aryl protons on two different aromatic rings (δ 6.83, 6.63 ppm, 4H), (ii) the sets of signals for the methyl groups substituting the two different aryl groups (δ 2.23 and 2.20, 9H; δ 2.09 and 2.06 ppm, 9H), and (iii) an upfield singlet (δ 1.31 ppm, 3H), which represents the methyl group added to the imine carbon and is now part of a d_3-*gem* dimethyl group. The deuterium labels of **14**-$d_6\cdot Et_2O$ can be observed directly in the ^2H NMR spectrum at δ 2.2 and 1.3 ppm.

For the mesityl-substituted DAB (2,4,6-$Me_3C_6H_2$)N=C(Me)C(Me)=N(2,4,6-$Me_3C_6H_2$) (**8**), the backbone methyl protons are sufficiently acidic to be abstracted by added MeLi to give **15**$\cdot Et_2O$; however, for the deuterated analogue **8**-d_6, proton (or more precisely deuteron) abstraction is turned off and nucleophilic attack at the imine carbon is the preferred reaction pathway. It is reasonable to conclude then that there are two competing reaction pathways for the reaction of diacetyl-based DABs with MeLi: (i) proton abstraction from the methyl group or (ii) nucleophilic methylation at the imine carbons. The reactions are similar in energy, with proton abstraction being the kinetically favored pathway, but factors which make this pathway more difficult (such as deuteration, steric loading, and the introduction of electron-rich substituents) switch the reaction to make nucleophilic addition the preferential pathway.

3. Conclusion

Selected diazabutadiene ligands derived from diacetyl were selectively reduced by lithium reagents to give new anionic ligands. Both MeLi and Bu^nLi can react with *N*,*N*′-(2,6-$Pr^i_2C_6H_3$)$_2$-1,4-diaza-2,3-dimethyl-1,3-butadiene (**7**) by nucleophilic attack at one of the imine carbon atoms. In contrast, with *N*,*N*′-(2,4,6-$Me_3C_6H_2$)$_2$-1,4-diaza-2,3-dimethyl-1,3-butadiene (**8**), MeLi acts simply as a base and abstracts a proton from one of the methyl groups attached to the imine carbon. The kinetic acidity of the protons attached to the imine carbon is the likely factor which determines whether reaction with alkyllithiums occurs by nucleophilic attack or with proton abstraction. Both deuteron incorporation and steric loading serve to decrease the kinetic acidity of the starting imine, and this in turn makes it more susceptible to a MeLi nucleophile. Both lithiated species, (2,6-$Pr^i_2C_6H_3$)N=C(Me)C(CH_3)$_2$N(Li)(2,6-$Pr^i_2C_6H_3$) (**13**) and (2,4,6-$Me_3C_6H_2$)N=C(Me)C(CH_3)$_2$N(Li)(2,4,6-$Me_3C_6H_2$) (**14**), have the potential to be useful ligands for stabilizing transition-metal centers. Preliminary reactions with a range of selected metal precursors are underway.

4. Experimental Section

Unless otherwise stated, all experiments and manipulations have been performed under an atmosphere of pure argon or dinitrogen by Schlenk and cannula techniques. The DAB ligands used in this work were prepared according to the literature.[9] Small quantities of diacetyl-d_6 were prepared by the literature method[17] and used to prepare (2,4,6-$Me_3C_6H_2$)N=C(CD_3)C(CD_3)=N(2,4,6-$Me_3C_6H_2$) (**8**-d_6) by standard means.[3] All solvents were dried over and distilled from appropriate drying agents and degassed after distillation. MeLi and MeLi·LiBr were obtained from Aldrich or Fisher in ether solution; Bu^nLi was obtained from Fisher in hexanes. Concentrations of the alkyllithium solutions were assessed by integration of the ^1H NMR spectra of known volumes against accurate masses of 1,5-cyclooctadiene;[18] a trace of benzene-d_6 was added to the solutions to facilitate assignment. ^1H and $^{13}C\{^1H\}$ NMR spectra were obtained on a Bruker Avance III 400 instrument operating at 400.13 and 100.61 MHz, respectively; $^2H\{^1H\}$ NMR spectra were obtained on a Bruker Avance II 300 instrument operating at 46.1 MHz. NMR spectra were referenced to the residual solvent resonances. X-ray diffraction experiments for **13**$\cdot Et_2O$ and and **15**−**18**$\cdot Et_2O$ were performed on a Bruker Kappa APEX-II CCD instrument at 150 K with graphite-monochromated Mo Kα radiation (λ = 0.710 75 Å). All crystals, mounted on the goniometer with cryo loops for intensity measurements, were coated with Paratone-N oil and then quickly transferred to the cold stream maintained by an Oxford Cryo stream attachment. Symmetry-related absorption corrections were applied by the SADABS program,[19] and the data were corrected for Lorentz and polarization effects with the Bruker APEX2 software suite.[19,20] All structures were solved by direct methods, and full-matrix least-squares refinements were carried out with SHELXL.[21] Three of the crystals (**13**$\cdot Et_2O$, **17**$\cdot Et_2O$, and **18**$\cdot Et_2O$) contain two crystallographically independent molecules in their asymmetric units, and almost all the structures gave rise to either rotational disorder in the isopropyl groups or conformational disorder in the coordinated diethyl ether molecule or in both positions. In each case, the disordered groups were refined using PART instruction and their geometries and thermal parameters were restrained by means of the DFIX, DELU, and SIMU options available in SHELXL.[21] Structure solution and refinement of **17**$\cdot Et_2O$ was attempted in tetragonal ($P4_3$), orthorhombic ($P2_12_12_1$), and monoclinic ($P2_1$) space groups, with the same cell parameters. On the basis of refinement parameters (lowest *R* value, 0.16), geometry of molecules, and behavior of anisotropic thermal parameters of atoms, the monoclinic space group $P2_1$ was adopted. An examination of reciprocal lattice plots indicated the possibility of twinning in these crystals, which could give rise to higher (pseudo) symmetry. In all cases, the non-hydrogen atoms were refined anisotropically. The hydrogen atoms, located in the difference Fourier maps, were refined isotropically under the riding model option in SHELXL.[21] The details of the crystal parameters, data collection, and refinements are summarized in Table 2. The Supporting Information contains CIF files for all the crystallographic data.

(2,6-$Pr^i_2C_6H_3$)N=C(Me)C(Me)$_2$N(Li)(2,6-$Pr^i_2C_6H_3$) (13$\cdot$**Et$_2$O).** MeLi in Et_2O (1.4 mL, 1.50 mol L^{-1} MeLi in Et_2O, 1.1 equiv) was added to a solution of (2,6-$Pr^i_2C_6H_3$)N=C(Me)C(Me)=N(2,6-$Pr^i_2C_6H_3$) (**7**; 0.777 g, 1.92×10^{-3} mol) in Et_2O (20 mL) at ice-bath temperature. The yellow color of the initial solution intensified, and an exotherm was noted. The solution was warmed to room temperature, filtered, and concentrated to 7 mL. The solution deposited yellow crystals of **13**$\cdot Et_2O$ upon standing at −15 °C (0.721 g, 75% yield). Anal. Calcd for $C_{33}H_{53}LiN_2O$: C, 79.16; H, 10.67; N, 5.60. Found: C, 79.00; H, 10.91; N, 5.50. ^1H NMR (400.13 MHz, 300 K, THF-d_8): δ 7.14, 6.85 (d, 4H, aryl, $^3J_{H,H'}$ = 8.0 Hz), 7.06, 6.59 (t, 2H, aryl, $^3J_{H,H'}$ = 8.0 Hz), 4.23, 3.06 (sept, 4H, C*H*(CH_3)$_2$, $^3J_{H,H'}$ = 6.8 Hz), 3.39 (q, 4H, OC*H*$_2$CH$_3$, $^3J_{H,H'}$ = 7.0 Hz), 1.81 (s, 3H, C*H*$_3$C=N), 1.30 (s, 6H, (C*H*$_3$)$_2$CN), 1.20, 1.18 (d, 24H, CH(C*H*$_3$)$_2$, $^3J_{H,H'}$ = 6.8 Hz), 1.10 (t, 6H, OCH$_2$C*H*$_3$, $^3J_{H,H'}$ = 7.0 Hz). $^{13}C\{^1H\}$ NMR (100.61 MHz, 300 K, THF-d_8): δ 193.8 (*C*=N), 158.0, 149.0, 147.4, 138.9, 124.9, 124.1, 122.3, 118.3 (*aryl*), 68.4 (*C*(CH_3)$_2$N), 66.4 (O*C*H$_2$), 31.1, 28.5, 28.0, 24.4, 24.3, 18.7 (peak assignment is ambiguous due to coincidence of chemical shifts), 15.8 (OCH$_2$*C*H$_3$).

(2,4,6-$Me_3C_6H_2$)N=C(CD_3)C(CD_3)(Me)N(Li)(2,4,6-$Me_3C_6H_2$) (14-$d_6\cdot Et_2O$). An ether solution of MeLi (1.9 mL, 1.0 mol L^{-1} MeLi

(18) Hoye, T. R.; Eklov, B. M.; Voloshin, M. *Org. Lett.* **2004**, *6*, 2567–2570.

(19) *SADABS*; Bruker Analytical X-ray Instruments Inc., Madison, WI, 2001.

(20) *SAINT*; Bruker Analytical X-ray Instruments Inc., Madison, WI, 2007.

(21) Sheldrick, G. M. *Acta Crystallogr., Sect. A* **2008**, *64*, 112–122.

Table 2. Crystal and Refinement Data for (2,6-Pr$^i_2$C$_6$H$_3$)N=C(Me)C(CH$_3$)$_2$N(Li)(2,6-Pr$^i_2$C$_6$H$_3$) (13·Et$_2$O), (2,4,6-Me$_3$C$_6$H$_2$)N=C(Me)C(=CH$_2$)N(Li)(2,4,6-Me$_3$C$_6$H$_2$) (15·Et$_2$O), (2,4,6-Me$_3$C$_6$H$_2$)(Li)NC(=CH$_2$)C(=CH$_2$)N(Li)(2,4,6-Me$_3$C$_6$H$_2$) (16·(Et$_2$O)$_3$(LiBr)$_2$), and (2,6-Pr$^i_2$C$_6$H$_3$)N=C(Me)C(=CH$_2$)N(Li)(2,6-Pr$^i_2$C$_6$H$_3$), (17·Et$_2$O)

	13·Et$_2$O	15·Et$_2$O	16·3Et$_2$O·2LiBr	17·Et$_2$O
empirical formula	$C_{33}H_{53}LiN_2O$	$C_{26}H_{37}LiN_2O$	$C_{17}H_{23}Br_2Li_2NO_{3/2}$	$C_{32}H_{49}LiN_2O$
fw	500.73	400.53	359.15	484.69
T, K	150(2)	150(2)	150(2)	150(2)
a, Å	33.1529(10)	16.436(3)	9.3319(4)	10.017(14)
b, Å	9.7406(3)	8.7758(17)	22.4980(10)	30.64(6)
c, Å	19.9215(6)	17.154(4)	10.1430(4)	10.062(13)
α, deg	90.00	90.00	90.00	90.00
β, deg	92.984(2)	90.00	112.340(2)	90.00
γ, deg	90.00	90.00	90.00	90.00
V, Å^3	6424.5(3)	2474.3(9)	1969.68(14)	3089(9)
Z	8	4	4	4
cryst syst	monoclinic	orthorhombic	monoclinic	monoclinic
space group	$P2_1/c$	$Pca2_1$	$P2_1/m$	$P2_1$
d_{calcd}, g cm^{-3}	1.035	1.075	1.211	1.042
θ range, deg	2.328−21.708	2.63−19.16	2.352−29.125	2.454−20.183
μ, mm^{-1}	0.061	0.064	2.088	0.061
GOF[a]	1.012	0.869	1.068	2.023
R1[b], wR2[c] [($I > 2\sigma(I)$)]	0.0601, 0.1399	0.0614, 0.1414	0.0350, 0.0873	0.1633, 0.2126
R1, wR2 (all data)	0.1093, 0.1669	0.1641, 0.1950	0.0457, 0.0930	0.3774, 0.3952

[a] GOF = $[\sum w(|F_o| - |F_c|)^2/(N_{obs} - N_{param})]^{1/2}$. [b] R1 = $\sum||F_o| - |F_c||/\sum|F_o|$. [c] wR2 = $[\sum w(|F_o^2| - |F_c^2|)^2/\sum w|F_o^2|^2]^{1/2}$.

in Et$_2$O, 1.1 equiv) was added to a slurry of (2,4,6-Me$_3$C$_6$H$_2$)N=C(CD$_3$)C(CD$_3$)=N(2,4,6-Me$_3$C$_6$H$_2$) (**8**-d_6; 0.567 g, 1.74 × 10^{-3} mol) in Et$_2$O (20 mL) at ice-bath temperature. The slurry dissolved to give a clear, yellow solution, and after 10 min, a yellow solid deposited. Et$_2$O was removed under reduced pressure, and the residue was redissolved in THF (5 mL) to give a bright yellow solution that was layered with hexanes (10 mL). The mixture was allowed to stand at −15 °C, and yellow crystals appeared (0.250 g, 34% yield). Anal. Calcd for $C_{27}H_{35}D_6LiN_2O$: C, 76.74; H, 8.35; N, 6.63. Found: C, 77.05; H, 9.00; N, 6.73. ^{1}H NMR (400.13 MHz, 300 K, THF-d_8): δ 6.83, 6.63 (s, 4H, *aryl*), 3.39 (q, 4H, OCH_2CH$_3$, $^3J_{H,H'}$ = 7.0 Hz), 2.23 (s, 6H, CH_3), 2.20 (s, 3H, CH_3'), 2.09 (s, 3H, CH_3), 2.06 (s, 6H, CH_3'), 1.31 (s, 3H, CD$_3$CH_3), 1.10 (t, 6H, OCH$_2$CH_3, $^3J_{H,H'}$ = 7.0 Hz). ^{13}C{^{1}H} NMR (100.61 MHz, 300 K, THF-d_8): δ 193.7 (*C*=N), 147.9, 135.7, 132.4, 131.5, 129.6 129.0, 128.7 127.7 (*aryl*), 69.1 (*C*(CH$_3$)$_2$N), 66.5 (O*C*H$_2$), 32.0 (CD$_3$*C*H$_3$), 22.7, 21.2, 21.0, 18.7 (*C*H$_3$), 15.9 (OCH$_2$*C*H$_3$). ^{2}H{^{1}H} NMR (46.1 MHz, 300 K, THF/hexanes): δ 2.20 (s, N=CC*D*$_3$), 1.3 (s, N−C(CH$_3$)(C*D*$_3$)).

(2,4,6-Me$_3$C$_6$H$_2$)N=C(Me)C(=CH$_2$)N(Li)(2,4,6-Me$_3$C$_6$H$_2$) (15·Et$_2$O). An ether solution of MeLi (12.9 mL, 1.0 mol L^{-1} MeLi in Et$_2$O, 1.05 equiv) was added to a slurry of (2,4,6-Me$_3$C$_6$H$_2$)N=C(Me)C(Me)=N(2,4,6-Me$_3$C$_6$H$_2$) (**8**; 10 g, 0.0128 mol) in Et$_2$O (40 mL) at ice-bath temperature. The slurry dissolved as the MeLi was added, and a clear, orange solution was obtained. The solution was stirred for 4 h and then concentrated to 15 mL. Upon standing at −5 °C, yellow crystals of (2,4,6-Me$_3$C$_6$H$_2$)N=C(Me)C(=CH$_2$)N(Li)(2,4,6-Me$_3$C$_6$H$_2$) (**15**·Et$_2$O) were deposited (3.05 g, 60% yield). Anal. Calcd for $C_{26}H_{37}LiN_2O$: C, 77.97; H, 9.31; N, 7.00. Found: C, 78.16; H, 9.02; N, 6.70. ^{1}H NMR (400.13 MHz, 300 K, THF-d_8): δ 6.84, 6.77 (s, 4H, *aryl*), 3.79, 2.96 (s, 2H, =CH_2), 3.38 (q, 4H, OCH_2CH$_3$, $^3J_{H,H'}$ = 7.0 Hz), 2.23 (s, 3H, CH_3), 2.14 (s, 6H, CH_3'), 2.15 (s, 3H, CH_3C=N), 2.04 (s, 6H, CH_3'), 1.91 (s, 3H, CH_3), 1.10 (t, 6H, OCH$_2$CH_3, $^3J_{H,H'}$ = 7.0 Hz). ^{13}C{^{1}H} NMR (100.61 MHz, 300 K, THF-d_8): δ 176.6 (*C*=N), 155.9, 154.0, 147.9, 132.5, 129.3, 128.9, 127.7, 126.9 (*aryl*), 76.0 (C=*C*H$_2$), 64.3 (O*C*H$_2$), 59.1 (*C*=CH$_2$), 43.8 (*C*H$_3$C=N), 26.6, 26.4, 22.3, 22.2, 18.7 (*C*H$_3$), 15.9 (OCH$_2$*C*H$_3$).

(2,4,6-Me$_3$C$_6$H$_2$)(Li)NC(=CH$_2$)C(=CH$_2$)N(Li)(2,4,6-Me$_3$C$_6$H$_2$) (16·3Et$_2$O·2LiBr). An ether solution of MeLi·LiBr (15.0 mL, 0.89 mol L^{-1} MeLi in Et$_2$O, 2.3 equiv) was added to a slurry of (2,4,6-Me$_3$C$_6$H$_2$)N=C(Me)C(Me)=N(2,4,6-Me$_3$C$_6$H$_2$) (**8**; 1.85 g, 5.77 × 10^{-3} mol) in Et$_2$O (60 mL) at ice-bath temperature. The yellow starting material dissolved to give a caramel-colored solution, from which an ocher material precipitated after 20 min. The slurry was stirred overnight, and volatiles were removed under reduced pressure. The ocher residue was recrystallized from Et$_2$O (15 mL), from which ocher crystals of (2,4,6-Me$_3$C$_6$H$_2$)(Li)NC(=CH$_2$)C(=CH$_2$)N(Li)(2,4,6-Me$_3$C$_6$H$_2$) (**16**·3Et$_2$O·2LiBr) were deposited (2.32 g, 55% yield). Anal. Calcd for $C_{30}H_{46}Br_2Li_4N_2O_2$: C, 55.19; H, 7.11; N, 4.29. Found: C, 55.30; H, 7.18; N, 4.32. ^{1}H NMR (400.13 MHz, 300 K, THF-d_8): δ 6.62 (s, 4H, *aryl*), 3.38 (q, 8H, OCH_2CH$_3$, $^3J_{H,H'}$ = 7.0 Hz), 3.08 (s, 2H, C=C*H*H′), 2.19 (s, 12H, CH_3), 2.14 (s, 6H, CH_3'), 2.13 (s, 2H, C=CH*H*′), 1.10 (t, 12H, OCH$_2$CH_3, $^3J_{H,H'}$ = 7.0 Hz). ^{13}C{^{1}H} NMR (100.61 MHz, 300 K, THF-d_8): δ 153.7, 131.6, 129.0, 126.1 (*aryl*), 66.4 (O*C*H$_2$CH$_3$), 58.6 (C=*C*H$_2$, quaternary vinyl could not be located), 21.2 (*p*-Me), 19.8 (*o*-Me), 15.8 (OCH$_2$*C*H$_3$).

(2,6-Pr$^i_2$C$_6$H$_3$)N=C(Me)C(=CH$_2$)N(Li)(2,6-Pr$^i_2$C$_6$H$_3$), (17·Et$_2$O). An ether/hexane solution of Pr$^i_2$NLi (prepared from 5.0 mL of a 1.57 mol L^{-1} Bu^{n}Li solution in hexanes added to 1.1 mL of Pr$^i_2$NH in 20 mL of Et$_2$O at −50 °C, 1.1 equiv) was added to a solution of (2,6-Pr$^i_2$C$_6$H$_3$)N=C(Me)C(Me)=N(2,6-Pr$^i_2$C$_6$H$_3$) (**7**; 2.88 g, 7.12 × 10^{-3} mol) in Et$_2$O (50 mL) at ice-bath temperature, and the mixture was warmed to room temperature. The solution became a more intense yellow, and the solution was stirred overnight. The solution was concentrated to a 10 mL volume, and yellow crystals of (2,6-Pr$^i_2$C$_6$H$_3$)N=C(Me)C(=CH$_2$)N(Li)(2,6-Pr$^i_2$C$_6$H$_3$) (**17**·Et$_2$O) appeared after standing at 5 °C (2.20 g, 65% yield). Anal. Calcd for $C_{32}H_{49}LiN_2O$: C, 79.30; H, 10.19; N, 5.78. Found: C, 79.50; H, 10.01; N, 6.00. ^{1}H NMR (400.13 MHz, 300 K, THF-d_8): δ 7.17, 6.95 (d, 4H, aryl, $^3J_{H,H'}$ = 7.8 Hz), 7.07, 6.75 (t, 2H, aryl, $^3J_{H,H'}$ = 7.8 Hz), 3.94, 3.14 (s, 2H, C=C*HH*′), 3.51, 3.04 (sept, 4H, C*H*(CH$_3$)$_2$, $^3J_{H,H'}$ = 6.8 Hz), 3.39 (q, 4H, OCH_2CH$_3$, $^3J_{H,H'}$ = 7.0 Hz), 2.02 (s, 3H, CH_3C=N), 1.20, 1.16, 1.12, 0.98 (d, 24H, CH(CH_3)$_2$, $^3J_{H,H'}$ = 6.8 Hz), 1.10 (t, 6H, OCH$_2$CH_3, $^3J_{H,H'}$ = 7.0 Hz). ^{13}C{^{1}H} NMR (100.61 MHz, 300 K, THF-d_8): δ 175.3 (*C*=N), 157.5, 141.9, 136.7, 122.8, 121.9, 121.1, 118.3, 117.5 (*aryl*), 78.0 (*C*=CH$_2$), 64.2 (O*C*H$_2$), 59.1 (C=*C*H$_2$), 44.0 (N=C*C*H$_3$), 26.7, 26.4, 23.7, 23.0 (CH(*C*H$_3$)$_2$), 22.3, 22.2 (*C*H(CH$_3$)$_2$), 15.8 (OCH$_2$*C*H$_3$).

(2,6-Pr$^i_2$C$_6$H$_3$)N=C(Me)C(Me)(C$_4$H$_9$)N(Li)(2,6-Pr$^i_2$C$_6$H$_3$) (18·Et$_2$O). Bu^{n}Li in hexanes (7.25 mL, 1.5 mol L^{-1} Bu^{n}Li in hexanes,1.05 equiv) was added to a slurry of (2,6-Pr$^i_2$C$_6$H$_3$)N=C(Me)C(Me)=N(2,6-Pr$^i_2$C$_6$H$_3$) (**7**; 4.16 g, 10.3 × 10^{-3} mol)

in Et_2O (50 mL) at ice-bath temperature. The resultant orange solution was concentrated to 40 mL and filtered from the residue, and orange and yellow crystals deposited at 5 °C. While an orange crystal corresponding to (2,6-$Pr^i_2C_6H_3$)N=C(Me)C(Me)(C_4H_9)N(Li)(2,6-$Pr^i_2C_6H_3$) (**18**·Et_2O) was selected for X-ray diffraction and characterized by these means, ^{1}H NMR spectroscopy revealed the presence of signals attributable to **17**·Et_2O, and no further characterization was attempted.

Supporting Information Available: CIF files giving crystallographic data for **13**·Et_2O and and **15**−**18**·Et_2O. This material is available free of charge via the Internet at http://pubs.acs.org.